ACS APPLIED MATERIALS & INTERFACES

Research Article

www.acsami.org

# Cellulose Nanocrystal/Silver Nanoparticle Composites as Bifunctional Nanofillers within Waterborne Polyurethane

He Liu,[†] Jie Song,[§] Shibin Shang,*[,†,‡] Zhanqian Song,*[,†,‡] and Dan Wang[†,‡]

[†]Institute of Chemical Industry of Forestry Products, CAF; Key Laboratory of Biomass Energy and Material, Jiangsu Province, P. R. China

National Engineering Laboratory for Biomass Chemical Utilization; Key Laboratory on Forest Chemical Engineering, SFA, Nanjing 210042, P. R. China

[‡]Institute of New Technology of Forestry, Chinese Academy of Forestry, Beijing 100091, P. R. China

[§]Department of Chemistry and Biochemistry, University of Michigan-Flint, Flint, Michigan 48502, United States

**ABSTRACT:** Developing bionanocomposites from renewable biomass is a viable supplement for materials produced from mineral and fossil fuel resources. In this study, nanocomposites composed of carboxylated cellulose nanocrystals (CCNs) and silver nanoparticles (AgNPs) were prepared and used as bifunctional nanofillers to improve the mechanical and antimicrobial properties of waterborne polyurethane (WPU). Morphology, structure and performance of the CCNs/AgNPs nanocomposites and WPU-based films were investigated. WPU-based composite films were homogeneous and reinforced. The WPU/CCNs/AgNPs composite showed excellent antimicrobial properties in killing both Gram-negative *E. coli* and Gram-positive *S. aureus*. The CCNs/AgNPs nanocomposites could be applied as bifunctional nanofillers within WPU.

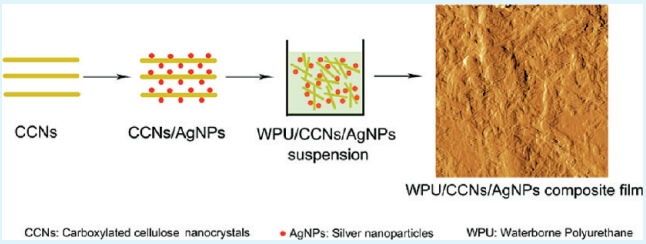


**KEYWORDS:** *cellulose nanocrystals, nanocomposites, waterborne polyurethane, nanofiller*

## INTRODUCTION

Biomass, as a viable supplement to fossil fuel resources, is an abundant carbon-neutral renewable resource available for the production of bioenergy and biomaterials. The use of biomass becomes more and more important and will be significant in addressing future human requirements.[1,2] Cellulose, the most abundant biomass carbon source, is a linear-chain carbohydrate polymer characterized by a high molecular weight homopolymer of $\beta$-1,4-linked anhydro-D-glucose units. Its characteristic solid-state and chemical properties are closely associated with its molecular structure. For example, its broad chemical variability results from the high donor reactivity of OH groups. Its OH functionality accounts for extensive hydrogen bonding networks, which gives cellulose a multitude of partially crystalline fiber structures.[3,4] Amorphous regions are present within solid-state cellulose and can be easily hydrolyzed by acid, whereas crystalline regions have a higher acid resistance.[4−6] Therefore, rodlike cellulose nanocrystals (CNs) can be produced by acid treatment. Currently, there is great interests in CNs because of their nanoscale dimensions, easy modification, abundant availability, high surface areas, unique morphology, low density, and low thermal-expansion mechanical strength;[5−15] these properties render CNs suitable for use within polymer matrices as a reinforcing nanofiller.[16−25]

Nanofillers consist of particles with at least one very small dimension when dispersed in polymers. A low volume fraction of nanofillers (like CNs) can significantly improve properties of polymer materials. However, monofunctional nanofiller can only improve a single property of host polymers. To prepare polymer materials with enhanced properties, mixtures of various nanofillers were used to blend with polymer matrices. Inorganic nanoparticles are important types of nanofillers that have been successfully used in the functionalization of polymer materials.[26] Inorganic nanoparticles bring new functionalities to the host polymer materials. However, the formation of aggregates or agglomerates will greatly reduce inorganic nanoparticles' applicability.[26] How to prepare inorganic nanoparticles without aggregation during their integration into the host polymer is a big challenge.

The synthesis of metallic nanoparticles is generally carried out by reducing metal salts in the presence of surfactants or polymeric ligands to passivate the cluster surface.[27] Most surfactants and polymeric ligands are prepared from nonrenewable petrochemicals, and finding a renewable biodegradable alternative is practically important because of exhausting fossil fuel resources. The use of cellulose-based materials as templates, scaffolds, and carriers in preparing metallic nanomaterials has been widely investigated.[28−36] Considering the functional properties of CNs and metallic nanoparticles (MNPs), the future use of CNs/MNPs nanocomposites as

**Received:** January 5, 2012
**Accepted:** April 16, 2012
**Published:** April 16, 2012

  

**Scheme 1. Schematic Showing the Experimental Procedure for Preparing the CCNs/AgNP Composite, And Its Subsequent Incorporation into WPU.**

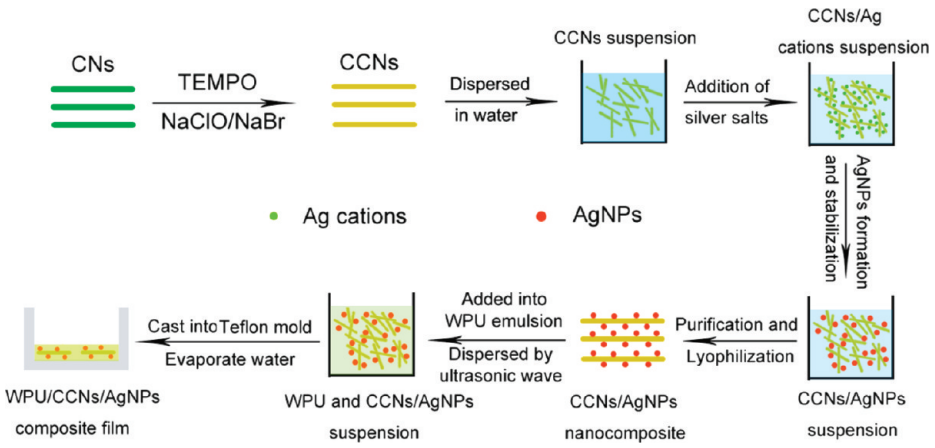


multifunctional nanofillers within polymer matrices is possible. The hydrophilic surface of CNs enables suitable blending with water based polymer matrices. Waterborne polyurethane (WPU) is a polymer commonly used in various products, including coatings, binders, adhesives, sealants, fibers, and foams. The improvement of WPU's mechanical and antimicrobial properties is valuable.[37]

In this study, nanocomposites composed of carboxylated cellulose nanocrystals (CCNs) and silver nanoparticles (AgNPs) were prepared and incorporated into WPU as nanofillers (scheme 1). CCNs were synthesized from CNs using the NaClO/NaBr/TEMPO (TEMPO, 2,2,6,6-tetramethylpiperidine-1-oxyl radical) oxidation system, and CCNs were then used as scaffolds and carriers for the stabilization of silver cations and AgNPs. AgNPs exhibit excellent antimicrobial properties and, therefore, the incorporation of the CCNs/AgNPs nanocomposites as bifunctional fillers in WPU is expected to improve WPU's mechanical and antimicrobial properties. WPU-based composites were prepared by casting and evaporating mixtures of CCNs/AgNPs and aqueous WPU suspensions in Teflon molds. The morphology, structure, and performance of the CCNs/AgNPs nanocomposites and WPU-based composite films were investigated and characterized.

## EXPERIMENTAL SECTION

**Materials.** Silver nitrate ($AgNO_3$), sulfuric acid ($H_2SO_4$, 98 wt %), sodium borohydride ($NaBH_4$), microcrystalline cellulose, sodium hypochlorite (NaClO), ethanol ($C_2H_5OH$), phosphotungstic acid hydrate ($H_3O_{40}PW_{12}\cdot H2O$), 2,2,6,6-tetramethylpiperidine-1-oxyl radical (TEMPO), sodium bromide (NaBr), sodium hydroxide (NaOH), polyether glycol (N-210; $\bar{M}_n$ =1000 g/mol), triethyl amine (TEA), Dimethylol propionic acid (DMPA), and diethylene glycol (DEG) were purchased from Sinopharm Chemical Reagent Co., Ltd. and used without further purification. 2,4-Toluene diisocyanate (TDI) was purchased from Jiangbei Chemical Reagents Factory (Wuhan, China) and redistilled before use.

**Preparation and Surface Modification of Cellulose Nanocrystals.** Cellulose nanocrystals powder was prepared by the acid-catalyzed hydrolysis of microcrystalline cellulose as previously described.[33,34] Microcrystalline cellulose (6 g) was mixed with sulfuric acid solution (90 mL, 64 wt %) and the mixture was stirred vigorously at 40 °C for 2 h. The suspension was then diluted ten times to stop the reaction. The suspension of pH 2 was obtained by centrifuging and washing the CNs suspension with water repeatedly. Dialysis was performed to remove free acid in the suspension, and the result was monitored by checking the neutrality of the dialysis effluent. CNs powder was finally freezing dried.

The carboxylation of CNs was carried out by NaClO/NaBr/TEMPO oxidation system.[38,39] Carboxylated CNs (CCNs) was prepared by the oxidation of CNs, which converts the surface primary hydroxyl groups to carboxylic acid groups via TEMPO-mediated carboxylation: 200 mL of 1 wt % CNs suspension was stirred slowly with 140 mg of TEMPO (70 mg/g CNs) and 360 mg of NaBr (180 mg/g CNs). An aliquot of 9 wt % NaClO solution was slowly added to the CNs suspension, and the pH was maintained at 10.5 at room temperature by adding NaOH over 10 h. The reaction was quenched with 30−40 mL of ethanol, and the product was purified by sequentially diluting with filtered deionized water and concentrated by ultrafiltration until the conductivity was ~100 $\mu$s/cm. CCNs powder was finally freeze-dried.

**Preparation of CCNs/AgNP Nanocomposites.** CCNs/AgNPs nanocomposites were prepared from the CCNs suspension by the reduction of silver cation. In a typical preparation, 1 mL of aqueous $AgNO_3$ ($1.0 \times 10^{-2}$ M) was added to the suspension (30 g, 1 wt %), followed by 1 h of stirring, CCNs/AgNPs gels were prepared by treating the suspension with 1 mL of $NaBH_4$ ($1.0 \times 10^{-2}$ M) solution at room temperature. After stirring for another 1 h, CCNs/AgNPs nanocomposites were then phase-separated from the suspension by centrifugation at 10 000 g. Under these conditions, CNs-based nanocomposites containing 0.357 wt % silver were prepared. Nanocomposites contained 1.766 wt % (5 mL, $AgNO_3$), 3.471 wt % (10 mL, $AgNO_3$), and 6.709 wt % (20 mL, $AgNO_3$) silver were also prepared under similar conditions.

**Synthesis of WPU.** WPU emulsion was prepared as previously described.[20,37] Polyether glycol N-210 (25.0 g) was added into a 250 mL four-necked round-bottom flask fitted with a mechanical stirrer, thermometer, reflux condenser and nitrogen inlet. The reaction was carried out at 110 °C for 3 h at reduced pressure to remove the water. The resulting prepolymer was cooled to 85 °C, and TDI (13.5 g) and DMPA (2.2 g) were poured into the flask while acetone was slowly added to obtain a homogeneous mixture, which was then allowed to react at 85 °C for 3 h. The prepolymer was extended by the addition of DEG (2.5 g), and allowed to react at 60 °C for 3 h, before being neutralized by the addition of TEA under stirring at 30 °C for 30 min. Dispersion was accomplished by slowly adding water to the neutralized PU solution under vigorous stirring. After removing the acetone (rotary evaporated under reduced pressure at 35 °C), the WPU emulsion with about 30 wt % solid content was obtained.

**Preparation of WPU/CCN and WPU/CCNs/AgNP Nanocomposite Films.** The WPU emulsion was mixed with a specific amount of aqueous CCNs and CCNs/AgNPs dispersion and sonicated for 20 min to obtain suspensions of different compositions. Resulting mixtures were stirred in a rotary evaporator under vacuum for 15 min to remove residual air and avoid the formation of

irreversible bubbles during evaporation. Resulting mixtures were subsequently cast in Teflon molds and water was removed by atmospheric evaporation at room temperature. The dry composite films were roasted at 50 °C for 5 h. A series of nanocomposite films with a thickness of ~0.3 mm were prepared by altering the CCNs content over the range of 0, 5, 10, 15, and 20 wt %, and are denoted as WPU, WPU/CCNs-5, WPU/CCNs-10, WPU/CCNs-15, and WPU/CCNs-20, respectively. CCNs/AgNPs nanocomposites with differing silver contents were mixed with WPU emulsions for preparing composite films which are denoted as WPU/CCNs-5/AgNPs-0.357, WPU/CCNs-5/AgNPs-1.766, WPU/CCNs-5/AgNPs-3.471, and WPU/CCNs-5/AgNPs-6.709. Prior to characterization, the resulting films were conditioned at room temperature in a desiccator containing $P_2O_5$ with 0% relative humidity (RH).

**Antibacterial Activity of WPU-Based Composite Films.** Antibacterial activity testing of WPU-based films was adopted from ASTM G 21−09 and previously reported studies.[37,40] Gram-negative *E. coli* and Gram positive *S. aureus* were selected for bactericidal testing. All glassware was sterilized in an autoclave at 120 °C for 30 min. Sample films of 50 mm ×50 mm were washed with 70 wt % ethanol to kill any residual surface bacteria, and then washed with sterilized water. 0.2 mL of bacterial suspension of 2.0−5.0 × $10^6$ colony forming units per mL (CFU/mL) was pipetted onto the surface of the dried film in a Petri dish and then covered with a PE film (40 mm ×40 mm). WPU-based films were incubated at RH > 90% and temperature of 37 °C for 24 h. Each WPU-based film was subsequently transferred to a new Petri dish and thoroughly washed with 20 mL of 0.87 wt % NaCl solution containing 0.03 wt % Tween 80 at pH 7.0. For determination of the actual number of microorganism colonies, the washing solution from each Petri dish was diluted to a series of lesser concentrations with sterile phosphate buffer saline. One mL of diluted solution was then spread onto a solid growth agar plate (containing 5 g/L beef extract, 10 g/L peptone, 5 g/L NaCl and 15 g/L agar powder). After incubation of the plates at 37 °C for 24 h, the number of viable microorganism colonies was counted manually, and the results after multiplication by dilution factor and averaging duplicate counts were expressed as mean CFU. The antibacterial ratio was calculated using:

$$\text{antibacterial ratio } (\%) = \frac{N_o - N}{N_o} \times 100\%$$

where, $N_o$ is the mean number of bacteria on the pure WPU film samples (CFU/sample), and N is the mean number of bacteria on the composite film samples (CFU/sample). Each sample was tested three times.

**ICP-OES Analysis of Silver in Washing Solution.** WPU composite films were immersed in 40 mL washing solutions with and without bacteria for 24 h in beakers. After washing solutions were evaporated, 5 mL $HNO_3$ (65 wt %) were added to the beakers and boiled for 20 min. Then the $HNO_3$ solutions were diluted with deionized water to volume 25 mL for inductively coupled plasma optical emission spectrometer (ICP-OES) analysis.

**Characterizations.** The morphology of CCNs and AgNPs was observed by transmission electron microscopy (TEM), using a JEOL 2100 microscope operating at 200 kV. TEM samples were typically prepared by dropping the sample suspension on a Cu grid coated with a carbon film, and TEM images of CCNs were obtained by staining using 1.0 wt % phosphotungstic acid. Fourier transform infrared (FT-IR) spectra were recorded on a iS10 FT-IR Spectrometer (Nicolet). The neat WPU film, WPU/CNs/AgNPs composite film, and a suspension of CNs/AgNPs were optically characterized using a Shimadzu 2550 UV−vis spectrophotometer. Atomic force microscopy (AFM) was carried out using a Shimadzu SPM9600, and used to investigate the surface of WPU-based films. The washing solutions of WPU/CCNs/AgNPs were analyzed with a PerkinElmer Optima 7000 ICP-OES. The mechanical properties of the WPU-based films were measured on a universal testing machine (CMT 6503, Shenzhen SANS Test Machine Co. Ltd., China) and an average value of at least five replicates for each sample was taken.

## RESULT AND DISCUSSION

**Characterization of CCNs.** A TEM image of CCNs deposited from a dilute suspension is shown in Figure 1, from

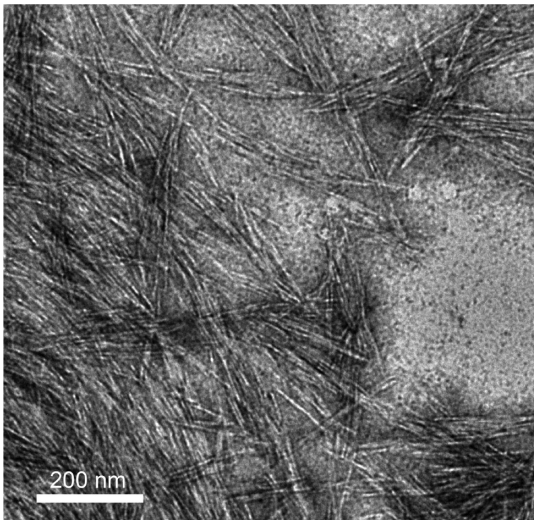


**Figure 1.** TEM image of CCNs.

which it is apparent the suspension contains cellulose fragments. Fragments appear as slender rods of ~10−20 nm in diameter and 100−200 nm in length. CCNs look bright in the TEM image due to their stained by phosphotungstic acid. Figure 2 shows the FT-IR transmission spectra of sulfuric acid

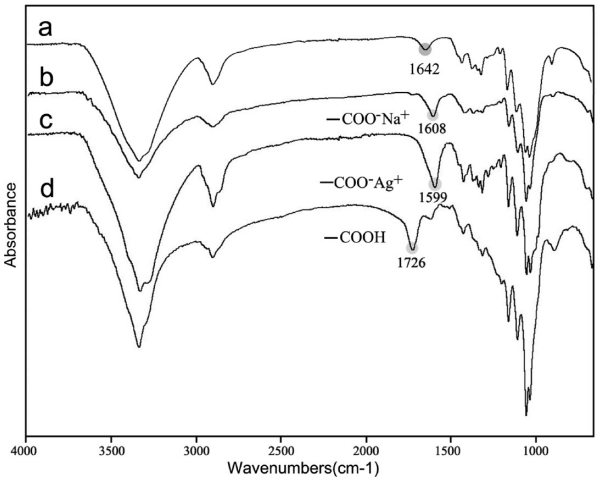


**Figure 2.** FT-IR transmission spectra: (a) CNs, (b) CCNs with sodium salt, (c) CCNs with silver salt, and (d) CCNs.

hydrolyzed CNs and CCNs. It confirms that the introduction of carboxylic acid groups is achieved by the TEMPO mediated oxidation of primary alcohol groups on the CNs surface. The spectrum of sulfuric acid hydrolyzed CNs (Figure 2a) shows a 1642 $cm^{-1}$ peak in the carbonyl region, presumably due to the partial oxidation of carbon on the cellulose backbone.[31] TEMPO mediated oxidation of primary alcohol groups on the CNs surface is characterized by a new carboxylic peak at 1726 $cm^{-1}$ (Figure 2d).[30] In the present study, the neutralized CCNs with NaOH show a 1608 $cm^{-1}$ peak, and after treated with $AgNO_3$ aqueous solution, the C═O vibration of the carboxylate anion shifts from 1608 to 1599 $cm^{-1}$, suggesting


dx.doi.org/10.1021/am3000209 | ACS Appl. Mater. Interfaces 2012, 4, 2413−2419

that silver salts are adsorbed on CCNs via $-COO^-$ (Figure 2b,c).[30]

**Morphology of AgNPs.** CCNs' strong ability to adsorb metallic cations is attributed to its abundant surface carboxyl and hydroxyl groups. After treating using $NaBH_4$ solution, the colorless $Ag^+$ on the CCNs turn to yellow upon reduction, indicating the formation of AgNPs. Carboxylate groups result in the high density immobilization of silver nanoparticles on CCNs.[30] CCNs/AgNPs suspensions redispersed in distilled water are found to be stable, with no obvious deposition or flocculation observed within 4 months. TEM images of AgNPs are listed in Figure 3, which show that nanostructures are

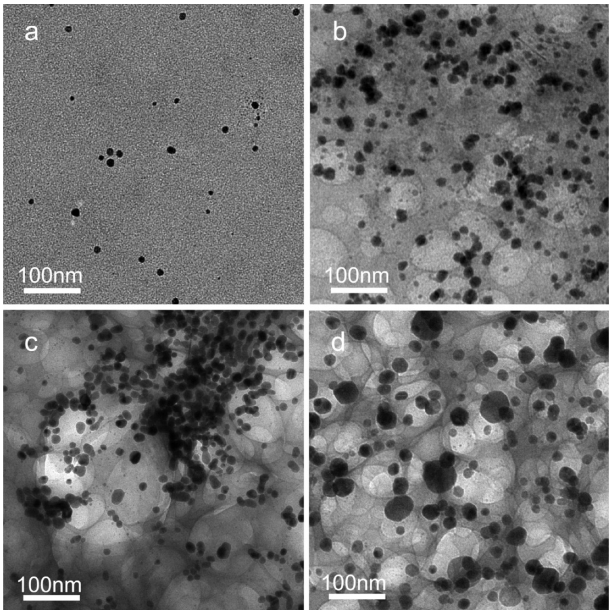


**Figure 3.** TEM images of AgNPs synthesized with different amounts of silver in the CCNs/AgNPs nanocomposites: (a) 0.357, (b) 1.766, (c) 3.471, and (d) 6.709 wt %.

formed in the CCNs suspension, and AgNPs are dispersed in the presence of CCNs. Due to their strong interactions with carboxyl and hydroxyl groups, silver cations are uniformly and tightly attached to CCNs.[28−30] Such interactions decrease mobility of silver cation, prevent the growth of large particles, and stabilize silver nanoparticles. TEM characterization of nanocomposites shows well-contrasted AgNPs because CCNs give little contrast against the resin.[28] Average size of AgNPs is less than 10 nm when silver content of silver is 0.357 wt % (Figure 3a). Increasing silver content to 1.766 and 3.471 wt % leads to most AgNPs with ∼15 nm in size (Figure 3b and Figure 3c). Sizes of AgNPs increases to more than 50 nm when silver content reaches 6.709 wt %. Average size of nanoparticles clearly increases with metal cation concentration during the synthesis.

**Morphology of WPU-Based Films.** Characterization of the upper surfaces of WPU, WPU/CNs-5 and WPU/CCNs-5/AgNPs-3.471 films was carried out by AFM. When films were cast in Teflon molds, the surfaces in contact with the atmosphere were denoted as the upper surfaces. The AFM images in Figure 4a show that the surface of the neat WPU film is rough, and no morphology due to CCNs is observed. In contrast, the rod-like morphology of CCNs is easily identified in Figure 4b. Our investigation indicates that no CCNs sedimentation or flocculation occurred during the evaporation process. Homogeneous distribution of CCNs in the WPU matrix is observed and implies there is good compatibility between the filler and polymeric matrix. In Figure 4c, morphology of CCNs is easily identified but AgNPs in the WPU/CCNs/AgNPs composite films are not apparent.

The optical properties of WPU/CCNs-5, CCNs/AgNPs-3.471 and WPU/CCNs-5/AgNPs-3.471 observed by UV−vis absorption spectrophotometry are shown in Figure 5. There is no absorption band found in the region of 350−600 nm for WPU/CCNs-5 (Figure 5a). In comparison, an absorption band at about ∼450 nm is observed for WPU/CCNs-5/AgNPs (Figure 5c). It is known that AgNPs exhibit a surface plasmon resonance band between 350 and 500 nm, and this is clearly evident for CCNs/AgNPs-3.471 in Figure 5b. Surface plasmon resonance band of WPU/CCNs-5/AgNPs is attributed to the presence of AgNPs. Compared with WPU/CCNs/AgNPs, CCNs/AgNPs shows no band shift due to surface plasmon resonance. It is a sign of the well-dispersed AgNPs within WPU matrices otherwise band shift will be caused by AgNPs' aggregation.[40,41] Figure 6 shows TEM images of AgNPs contained in the WPU-based films. The AgNPs in WPU/CCNs-5/AgNPs-1.766 (Figure 6a) and WPU/CCNs-5/AgNPs-6.709 (Figure 6b) are the samples shown in images b and d in Figure 3, respectively. It indicates that AgNPs contained in the WPU films are dispersed.

**Mechanical Properties.** The mechanical behavior of WPU films and composite films reinforced with various compositions of CCNs and CCNs/AgNPs nanocomposites were investigated by tensile testing at room temperature. Results of tensile strength and elongation at break are presented in Table 1 as a function of CCN and AgNP content for the WPU matrix composite films. Tensile strength improves from 15.2 to 33.7 MPa, which represents a ∼121% increase, upon increasing CCNs content from 0 to 10 wt % WPU. This indicates that incorporating CCNs into the WPU matrix results in strong interactions between the filler and matrix and, thus, restricts the matrix motion. Further addition of CCNs decreases tensile strength, but it still remains higher than that of the neat WPU film. This result disagrees with a previous report that tensile strength increase is continuous with increasing CCNs filler content up to 30 wt %.[20] The discrepancy may be explained by different WPU components and cellulose nanocrystals modification. In this study, TDI was a hard segment in the WPU matrix, whose stiffness makes the tensile strength of neat WPU higher than that reported by Cao et al.[20] In general, excessive CCNs may interrupt the original interactions between soft and hard segments. Elongation at break of WPU-based composite films decreased from 2041 to 1239% while CCNs filler content increases from 0 to 20 wt %. Tensile strength decreased significantly from 25.8 (sample WPU/CCNs-5) to ∼18.0 MPa with increasing AgNPs content, whereas elongation at break increased only slightly. This phenomenon may be caused by interaction of AgNPs with CCNs and WPU. The AgNPs reduce the interaction of the WPU matrix with the CCNs as many of the COOH groups are presumably complexed with the AgNPs. Thus, AgNPs reduce restriction of the matrix motion caused by CCNs.

**Antibacterial Activity of WPU/CCNs-5/Ag Composites.** The antibacterial activity of WPU/CCNs-5/AgNPs composite films with various silver contents was tested using *E. coli* and *S. aureus*, in comparison with the pure WPU, WPU/CCNs-5 film and WPU/CCNs-5/AgNPs composite films. Results are

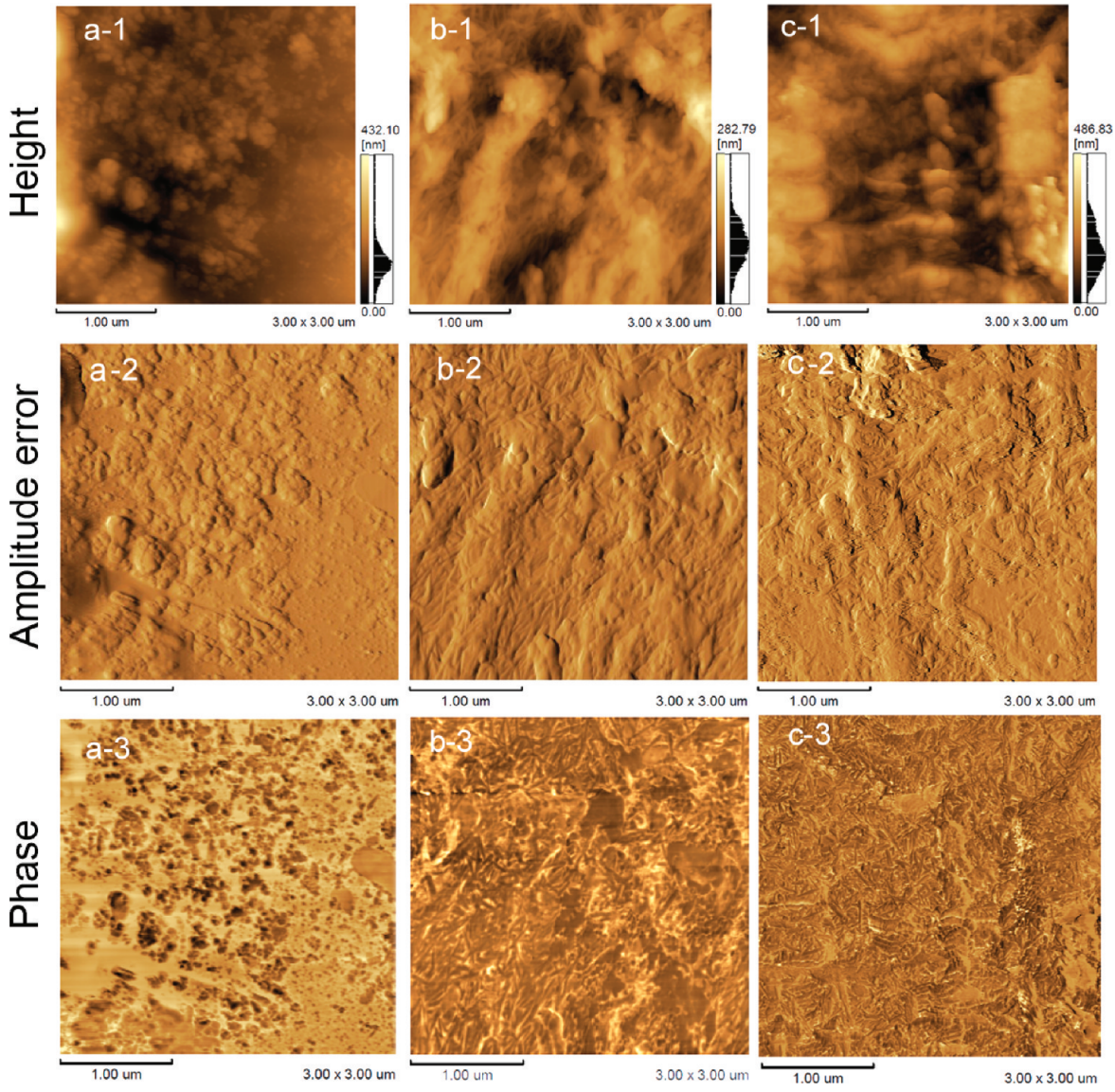


**Figure 4.** Different state type of AFM images of (a) WPU film, (b) WPU/CCNs-5 film, and (c) WPU/CCNs-5/AgNPs-3.471.

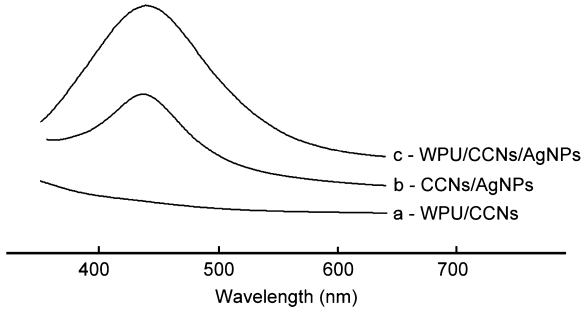


**Figure 5.** UV−vis spectra of (a) WPU/CCNs, (b) CCNs/AgNPs, and (c) WPU/CCNs/AgNPs.

displayed in Table 1. All WPU/CCNs-5/AgNPs composite films have strong and uniformed antibacterial activities to *E. coli*. The antibacterial activity of WPU/CCNs-5/AgNPs composite films to *S. aureus* is weaker than that to *E. coli*, and a fluctuation in antibacterial activity is observed with varying silver contents. Antibacterial mechanisms of silver nanoparticles remain unresolved but it is commonly believed that AgNPs interact with constituents of bacteria's outer membrane, causing structural changes and degradation that eventually lead to cell death.[40,42] AgNPs with a size less than 15 nm are well-known to have efficient antibacterial activity because they are able to penetrate inside the bacteria and cause further damages, possibly by interacting with sulfur- and phosphorus-containing moieties of DNA.[42−44] It is conjectured that antibacterial activities of WPU/CCNs-5/AgNPs result from altering the size of AgNPs by varying silver cation content in the synthesis process. Figure 3 indicates that the nanoparticles size increases with increasing silver cation content from 0.357 to 3.471 wt % (Figure 3a,c), but size of AgNPs is still less than 15 nm. The increasing silver content will increase the amount or the total surface area of AgNPs, which result in the improvement of WPU-based composites' antibacterial activity. When silver cation content is saturated, most particles become much larger than 15 nm (Figure 3d). Larger AgNPs would be unable to penetrate inside the bacteria, and thus reduce the antibacterial activity.

The long-term antibacterial activity of the WPU/CCNs/AgNPs films was also investigated. The antibacterial activity of

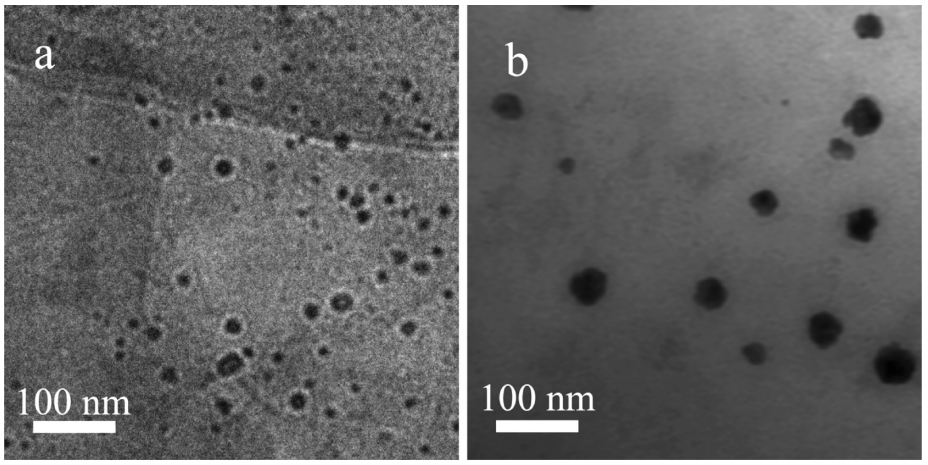


**Figure 6.** TEM images of AgNPs in WPU composites: (a) WPU/CCNs-5/AgNPs-1.766 and (b) WPU/CCNs-5/AgNPs-6.709.

**Table 1. Data Showing of WPU-Based Films: Tensile Strength ($\sigma_B$), Elongation at Break ($\varepsilon$), and Antibacterial Activity**

| sample | $\sigma_B$ (MPa) | $\varepsilon$ (%) | antibacterial ratio of *E. coli* (%) | antibacterial ratio of *S. aureus* (%) |
|---|---|---|---|---|
| WPU | 15.2 ± 0.7 | 2041 ± 61 | 0.0 | 0.0 |
| WPU/CCNs-5 | 25.8 ± 1.7 | 1751 ± 42 | 0.0 | 0.0 |
| WPU/CCNs-10 | 33.7 ± 1.6 | 1573 ± 51 | | |
| WPU/CCNs-15 | 27.3 ± 0.6 | 1454 ± 47 | | |
| WPU/CCNs-20 | 24.5 ± 1.3 | 1239 ± 57 | | |
| WPU/CCNs-5/Ag-0.357 | 21.0 ± 1.1 | 1740 ± 52 | 99.4 ± 0.1 | 76.4 ± 3.4 |
| WPU/CCNs-5/Ag-1.766 | 18.0 ± 1.9 | 1814 ± 44 | 99.2 ± 0.3 | 79.3 ± 6.0 |
| WPU/CCNs-5/Ag-3.471 | 17.7 ± 1.6 | 1833 ± 45 | 99.7 ± 0.3 | 86.0 ± 4.4 |
| WPU/CCNs-5/Ag-6.709 | 18.4 ± 1.7 | 1857 ± 36 | 97.5 ± 0.7 | 75.3 ± 5.9 |
| WPU/CCNs-5/Ag-3.471: the third time | | | 99.5 ± 0.4 | 87.7 ± 2.7 |
| WPU/CCNs-5/Ag-3.471: the fourth time | | | 97.2 ± 0.5 | 82.7 ± 3.2 |
| WPU/CCNs-5/Ag-3.471: the fifth time | | | 91.9 ± 2.5 | 67.8 ± 2.1 |

the WPU/CCNs/AgNPs films becomes weaker against bacteria after 3 cycles, which is showed in Table 1. This result may be caused by the escape of AgNPs from WPU matrix. The washing solutions of WPU/CCNs/AgNPs were detected by ICP-OES. Appearance of silver in washing solutions containing bacteria indicates that AgNPs are released from the composite film when bacteria are spread onto the composite film by some intermolecular force between AgNPs and membrane of bacteria. As established by the theory of hard and soft acids and bases, silver have a higher affinity to react with phosphorus and sulfur compounds which is well-known to be contained in many proteins of bacterial membrane.[43,45] These proteins might be preferential sites for the silver nanoparticles. The affinity between AgNPs and bacterial membrane is intensity. In previous investigation, AgNPs with negatively charged attached to the bacterial membrane by affinity, although the bacterial membrane were negatively charged.[42]

## CONCLUSION

CCN/AgNP nanocomposites were prepared, and morphology, mechanical behavior, and antibacterial activity of WPU-based composites and neat WPU were investigated. AFM and UV–vis results indicate that CCNs and AgNPs are dispersed homogeneously within the WPU matrix. However, AgNPs and CCNs show opposite effect on mechanical behavior. CCNs significantly increases tensile strength of WPU-based films to an optimum value (10 wt %) and then gradually decreases. In comparison, tensile strength of WPU-based films decreases with increasing silver content. The elongation at break decreases greatly with increasing CCNs content and increases slightly with increasing silver content. More importantly, WPU/CCNs/AgNPs composite films indicate a strong antibacterial activity against *E. coli* and *S. aureus*. The results indicate that CCNs/AgNPs nanocomposites as reinforcing and antibacterial nanofiller are valuable for the WPU applications.

## AUTHOR INFORMATION

### Corresponding Author

*Fax: +86 25 85482468 (Z.S.); +86 25 85482499 (S.S.). Tel: +86 25 85482468 (Z.S.); +86 25 85482499 (S.S.). E-mail: lhssxly@hotmail.com (Z.S.); shangsb@hotmail.com (S.S.).

### Notes

The authors declare no competing financial interest.

## ACKNOWLEDGMENTS

We gratefully acknowledge the financial support from the National Natural Science Foundation of China (Grant 31070519).

## REFERENCES

(1) Ragauskas, A. J.; Williams, C. K.; Davison, B. H.; Britovsek, G.; Cairney, J.; Eckert, C. A.; Frederick, Jr. W. J.; Hallett, J. P.; Leak, D. J.; Liotta, C. L.; Mielenz, J. R.; Murphy, R.; Templer, R.; Tschaplinski, T. *Science*, **2006**, *311*, 484–489.

(2) McKendry, P. *Bioresour. Technol.* **2002**, *83*, 37–46.

(3) Klemm, D.; Heublein, B.; Fink, H. P.; Bohn, A. *Angew. Chem., Int. Ed.* **2005**, *44*, 3358–3393.

(4) Habibi, Y.; Lucia, L. A.; Rojas, O. J. *Chem. Rev.* **2010**, *110*, 3479–3500.

(5) Matos Ruiz, M.; Cavaillé, J. Y.; Dufresne, A.; Gérard, J. F.; Graillat, C. *Compos. Interfaces* **2000**, *7*, 117–131.

(6) Anglès, M. N.; Dufresne, A. *Marcomolecules* **2001**, *34*, 2921–2931.

(7) Zhao, Q.; Wang, S.; Cheng, X.; Yam, R. C. M.; Kong, D.; Li, R. K. Y. *Biomacromolecules* **2010**, *11*, 1364−1369.
(8) Zoppe, J. O.; Habibi, Y.; Rojas, O. J.; Venditti, R. A.; Johansson, L. S.; Efimenko, K.; Österberg, M.; Laine, J. *Biomacromolecules* **2010**, *11*, 2683−2691.
(9) Filpponen, I.; Argyropoulos, D. S. *Biomacromolecules* **2010**, *11*, 1060−1066.
(10) Goetz, L.; Foston, M.; Mathew, A. P.; Oksman, K.; Ragauskas, A. J. *Biomacromolecules* **2010**, *11*, 2660−2666.
(11) Eichhorn, S. J.; Young, R. J.; Davies, G. R. *Biomacromolecules* **2005**, *6*, 507−513.
(12) Sturcova, A.; Davies, G. R.; Eichhorn, S. J. *Biomacromolecules* **2005**, *6*, 1055−1061.
(13) Podsiadlo, P.; Choi, S.; Shim, B.; Lee, J.; Cussihy, M.; Kotov, N. *Biomacromolecules* **2005**, *6*, 2914−2918.
(14) Azizi Samir, M. A. S.; Alloin, F.; Dufresne, A. *Biomacromolecules* **2005**, *6*, 612−626.
(15) Nishino, T.; Matsuda, I.; Hirao, K. *Macromolecules* **2004**, *37*, 7683−7687.
(16) Gao, Z.; Peng, J.; Zhong, T.; Sun, J.; Wang, X.; Yue, C. *Carbohyd. Polym.* **2012**, *87*, 2068−2075.
(17) Bulota, M.; Tanpichai, S.; Hughes, M.; Eichhorn, S. J. *ACS Appl. Mater. Interfaces* **2012**, *4*, 331−337.
(18) Pei, A.; Malho, J. M.; Ruokolainen, J.; Zhou, Q.; Berglund, L. A. *Macromolecules* **2011**, *44*, 4422−4427.
(19) Auad, M. L.; Mosiewicki, M. A.; Richardson, T.; Aranguren, M. I.; Marcovich, N. E. *J. Appl. Polym. Sci.* **2010**, *115*, 1215−1225.
(20) Wang, Y.; Tian, H.; Zhang, L. *Carbohyd. Polym.* **2010**, *80*, 665−671.
(21) Tang, L.; Weder, C. *ACS Appl. Mater. Interfaces* **2010**, *2*, 1073−1080.
(22) Cao, X.; Habibi, Y.; Lucia, L. A. *J. Mater. Chem.* **2009**, *19*, 7137−7145.
(23) Cao, X.; Dong, H.; Li, C. M. *Biomacromolecules* **2007**, *3*, 899−904.
(24) Auad, M. L.; Contos, V. S.; Nutt, S.; Aranguren, M. I.; Marcovich, N. E. *Polym. Int.* **2008**, *57*, 651−659.
(25) Marcovich, N. E.; Auad, M. L.; Bellesi, N. E.; Nutt, S. R.; Aranguren, M. I. *J. Mater. Res.* **2006**, *21*, 870−881.
(26) Althues, H.; Henle, J.; Kaskel, S. *Chem. Soc. Rev.* **2007**, *36*, 1454−1465.
(27) Ferrando, R.; Jellinek, J.; Johnston, R. L. *Chem. Rev.* **2008**, *108*, 845−910.
(28) Cai, J.; Kimura, S.; Wada, M.; Kuga, S. *Biomacromolecules* **2009**, *10*, 87−94.
(29) Shin, Y.; Bae, I.; Arey, B. W.; Exarhos, G. J. *J. Phys. Chem. C* **2008**, *112*, 4844−4848.
(30) Shinsuke, I.; Manami, T.; Minoru, M.; Hiroyuki, S.; Hiroyuki, Y. *Biomacromolecules* **2009**, *10*, 2714−2717.
(31) Shin, Y.; Bae, I. T.; Arey, B. W.; Exarhos, G. J. *Mater. Lett.* **2007**, *61*, 3215−3217.
(32) Shin, Y.; Blackwood, J. M.; Bae, I. T.; Arey, B. W.; Exarhos, G. J. *Mater. Lett.* **2007**, *61*, 4297−4300.
(33) Liu, H.; Wang, D.; Shang, S.; Song, Z. *Carbohydr. Polym.* **2011**, *83*, 38−43.
(34) Liu, H.; Wang, D.; Song, Z.; Shang, S. *Cellulose* **2011**, *18*, 67−74.
(35) Padalkar, S.; Capadona, J. R.; Rowan, S. J.; Weder, C.; Won, Y. H.; Stanciu, L. A.; Moon, R. J. *Langmuir* **2010**, *26*, 8497−8502.
(36) Drogat, N.; Granet, R.; Sol, V.; Memmi, A.; Saad, N.; Koerkamp, C. K.; Bressollier, P.; Krausz, P. *J. Nanopart. Res.* **2011**, *13*, 1557−1562.
(37) Ma, X. Y.; Zhang, W. D. *Polym. Degrad. Stab.* **2009**, *94*, 1103−1109.
(38) Sehaqui, H.; Mushi, N. E.; Morimune, S.; Salajkova, M.; Nishino, T.; Berglund, L. A. *ACS Appl. Mater. Interfaces* **2012**, *4*, 1043−1049.
(39) Saito, T.; Nishiyama, Y.; Putaux, J. L.; Vignon, M.; Isogai, A. *Biomacromolecules* **2006**, *7*, 1687−1691.
(40) Kumar, A.; Vemula, P. K.; Ajayan, P. M.; John, G. *Nat. Mater.* **2008**, *7*, 236−241.
(41) Zhang, J.; Roll, D.; Geddes, C. D.; Lakowicz, J. R. *J. Phys. Chem. B* **2004**, *108*, 12210−12214.
(42) Sondi, I.; Salopek-Sondi, B. *J. Colloid Interface Sci.* **2004**, *275*, 177−182.
(43) Morones, J. R.; Elechiguerra, J. L.; Camacho, A.; Holt, K.; Kouri, J. B.; Ramírez, J. T.; Yacaman, M. J. *Nanotechnology* **2005**, *16*, 2346−2353.
(44) Singh, M.; Singh, S.; Prasada, S.; Gambhir, I. S. *Dig. J. Nanomater. Bios.* **2008**, *3*, 115−122.
(45) Hatchett, D. W.; Henry, S. *J. Phys. Chem.* **1996**, *100*, 9854−9859.